Stress-induced martensitic transformation, twin boundary mobility and elastic properties of Fe_7Pd_3 ferromagnetic shape memory alloy thin films

A. J. Bischoff[a,b,1], A. Landgraf[a,1], S. G. Mayr[a,b,c]

[a] *Leibniz-Institut für Oberflächenmodifizierung (IOM), Permoserstr. 15, 04318 Leipzig, Germany*
[b] *Translationszentrum für Regenerative Medizin (TRM), Universität Leipzig, Philipp-Rosenthal-Str. 55, 04103 Leipzig, Germany*
[c] *Fakultät für Physik und Geowissenschaften, Universität Leipzig, Linnéstr. 5, 04103 Leipzig, Germany.*

Abstract

Within an in-situ study, we explore mechanical properties of Fe_7Pd_3 ferromagnetic shape memory alloy thin films. While performing tensile measurements on freestanding films, we accomplish to observe the appearance of twin boundaries due to the stress-induced austenite-martensite transition. Changing distances between twin boundaries during further straining indicate the growth of single variant regions at the expense of others. Young's moduli of 2.2 to 8.3 GPa were determined. For comparison, temperature dependent surface acoustic waves were applied on as-deposited films exhibiting much higher Young's moduli. These findings are discussed considering the influence of phase stability and phase transition characteristics.

Keywords: Ferromagnetic shape memory, martensitic phase transformation, twinning, Young's modulus

Ferromagnetic shape memory (FM) alloys are a captivating class of smart functional materials and very promising candidates for miniaturized actuation devices. Applying an external magnetic field, they feature reversible strains of

Email addresses: alina.bischoff@iom-leipzig.de (A. J. Bischoff), stefan.mayr@iom-leipzig.de (S. G. Mayr)

[1] A. J. Bischoff and A. Landgraf contributed equally to this work.

several percent due to the reorientation of twin variants in the martensitic phase [1]. In this context, the FM alloy Fe_7Pd_3 is of particular interest because of its high ductility, low brittleness [2] and biocompatibility [3], enabling its use in micromedicine.

To yield strains resulting from magnetically induced reorientation of twin variants, magnetic forces need to overcome the twinning stress σ_t. As magnetic anisotropy establishes an upper limit for this force, higher twinning stresses will prevent magnetostrain, while minimized twinning stresses are clearly favorable [4, 5]. Besides, mechanical stresses can yield to a stress-induced transformation from austenitic to martensitic phase. For the Fe-Pd system this was only reported for bulk polycrystalline samples consisting of 30.5 *at.* % Pd: Within measurements with a tensile testing machine it was found that lattice softening and the occurrence of stress-induced martensitic transformation caused decreasing Young's moduli upon cooling down towards the martensitic start temperature M_s [6].

Characterization of mechanical properties with respect to twin boundary mobility constitutes an integral part of suitability assessments of FM alloys. In fact, while bulk samples have been extensively characterized, the impact of open surfaces in miniaturized thin films is yet not fully understood. In this work, we present tensile tests on freestanding Fe_7Pd_3 thin films performed directly within a scanning electron microscope (SEM). This allowed live imaging of changes in the surface relief due to twin boundary motion or generation during superplastic deformation and the martensitic transition, respectively. While this addresses deformation beyond linear elasticity, the Young's modulus during linear response was studied in detail for freestanding and substrate-attached single as well as polycrystalline samples.

Sample preparation of single and polycrystalline 500 nm Fe_7Pd_3 thin films was achieved with molecular beam epitaxy, as described previously [7, 8]. The samples were grown on MgO(001) substrates and thermally oxidized Si wafers, respectively. The austenitic phase transformation temperature of the grown films is slightly above room temperature varying a few kelvins due to off-

stoichiometry and stresses [9]. Single crystalline samples for tensile experiments were subsequently detached from their substrates in a saturated sodium bicarbonate $NaHCO_3$ solution [10]. Afterwards, the samples were placed on a Deben MICROTEST 200N Tensile Stage, which is designed for compression and horizontal straining and is suited for usage within a SEM. The thin film was mounted either completely freestanding or for stability reasons underlaid with polyethylene plastic wrap. The jaws to which the sample is clamped are driven in opposite directions at a speed of 0.1 mm/min and the force experienced on the sample is measured every 0.1 s with a standard miniature load cell. For the complementary SEM measurements a Carl Zeiss Ultra 55 was utilized.

Young's moduli of films on substrates were assessed with a laser acoustic test system LAwave. Here, surface acoustic waves (SAW) are excited by a pulsed nitrogen laser and their amplitudes are measured time-resolved at varying distances by a piezoelectric transducer. Young's moduli are determined by applying theory of acoustic wave propagation together with sample details [11].

The specimens consisted of $24.6 - 31.9$ *at.* % Pd, as determined with energy dispersive x-ray spectroscopy. Phase of austenitic (A) and martensitic (M) samples was identified by x-ray diffraction (XRD) measured with a Seifert XRD 3003 PTS. Details on the analyzed samples are summarized in Table 2. The thickness of the films varies locally and reaches up to ≈ 620 nm, as determined with atomic force microscopy (AFM) using a Veeco Icon Dimension. Exact thickness values were obtained using profilometer measurements carried out with a Taylor Hopson Talystep.

To investigate the stress-induced martensitic phase transition, the freestanding sample A1 (dimension $\approx$ 3.8 x 5.0 mm^2) supported with plastic wrap was strained. The measured force elongation curve is shown in Figure 1. Letters mark interruptions of the deformation process for taking SEM pictures of the surface. The shifts in force at these points appear due to relaxation processes of the restrained film and plastic wrap. The force exhibits a linear increase in the beginning indicating elastic deformation of the sample. Between measurement points e and f, we observed a peak followed by further but less steep

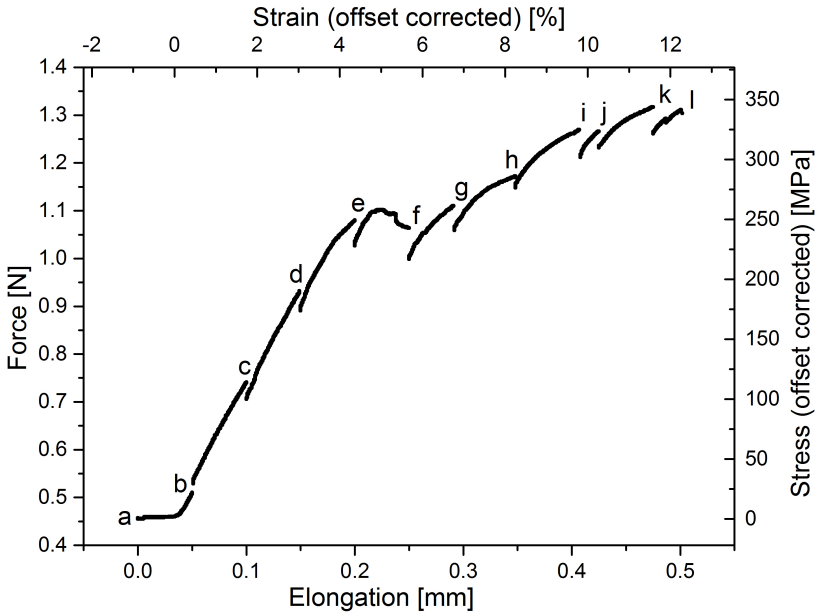

Figure 1: Force elongation curve of sample A1 with corresponding offset corrected stress and strain values.

increase until film rupture at point l. Test measurements with plastic wrap only revealed maximal stresses of $\approx$ 9 MPa in the strain range experienced by the thin film implying an insignificant stress contribution of the plastic wrap on the measurement.

In the linear elastic deformation regime from point a to e surface morphology resembled the substrate-attached sample (see Fig. 2a). It is characterized by groves between growth islands, but maintains an overall single crystalline-like morphology. At point f, the film surface changed considerably and twinning structures emerged (see Fig. 2b). This indicates a martensitic phase transition between the measurement points e and f, i.e. at strains between 4.4 and 5.7 % and at a maximal stress of $\approx$ 258.6 MPa (offset corrected). At this strain rate, the contribution of the plastic wrap is between 3.5 and 5.5 MPa meaning that the thin film experienced a maximal stress of 253.1 - 255.1 MPa.

This measured stress is about 50 % higher than the maximal stress of 170

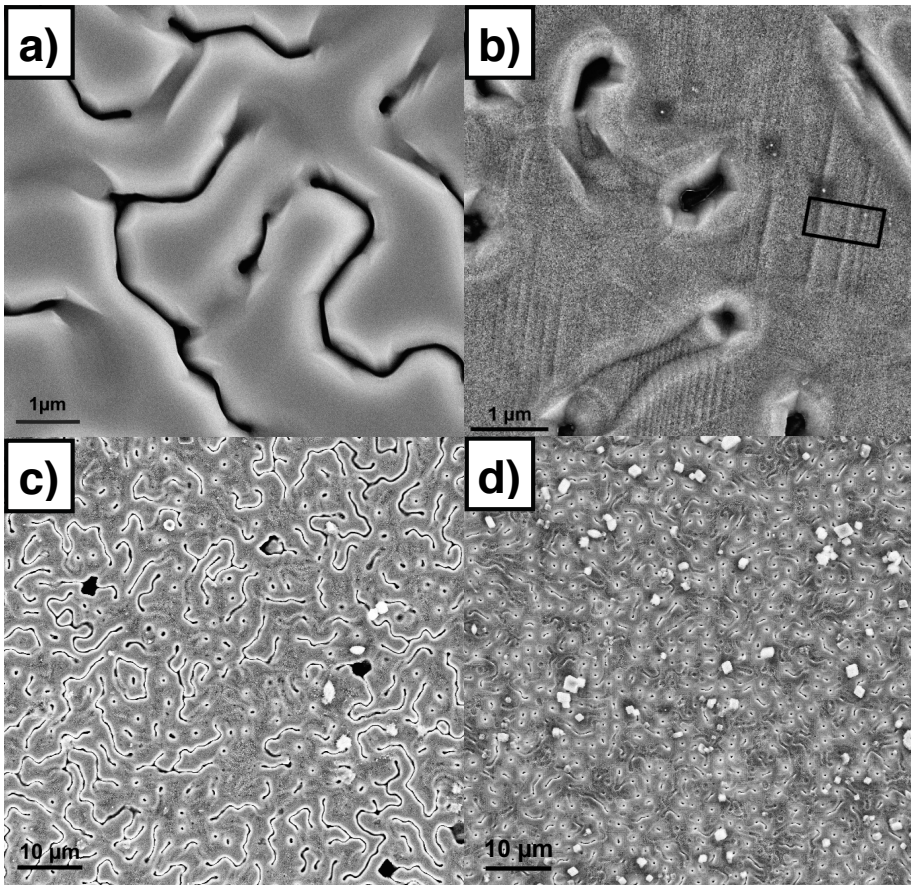

Figure 2: Preprocessed SEM pictures of different samples: A1 substrate-attached with no twinning structures on the surface (a), at point k on the force elongation curve with appeared twinning structures (b) and samples A3 (c) and A4 (d) before straining.

MPa which was necessary to complete the martensitic transformation in polycrystalline bulk samples at room temperature [6]. Compared to single crystals, induced martensitic transformation happens at lower stresses and faster in polycrystals because grain boundaries can function as nucleation sources for twinning dislocations enhancing the phase transition. Presence of open surfaces, on the other hand, might complicate nucleation due to image forces and roughening.

According to the Clausius-Clapeyron equation, the maximum applied stress during straining will shift the martensite temperature by up to 52 K which supports the observation of martensitic Fe_7Pd_3 at room temperature (calculation based on a typical martensite finish temperature of 273 K and other material characteristics as given in [6]).

Experimental verification of the phase change was established with XRD as shown in Figure 3. After straining, the freestanding, disrupted film showed two shoulders attached to the fcc peak at 48.70°. These two peaks at 47.85° and 49.68° are identified as the fct(200) and fct(002) peaks measured with a Rigaku Ultima IV. This exhibits that the fcc and fct structure coexist in the strained specimen. The remaining fcc fraction can be explained by possible pinning of twinning dislocations at defects, such as dislocations or the rough surface structure of the film [9]. Furthermore it is possible that the phase transition was not yet completed when the tensile measurement was stopped due to film rupture.

In order to investigate twin boundary mobility, changes in distances between single structures of the twinning relief during further straining of the film were examined. Therefore pictures of one particular region, which is marked in Figure 2b, were taken at different straining levels. On the basis of the grey value peaks corresponding to the locations of these surface structures in two pictures, the distances between individual twin boundaries were calculated. In each picture 40 profile cross sections were taken and the average peak positions for five neighboring structures of the twinning relief were determined. From left to right, these twin boundaries were denoted by the letters A to E. The obtained values for the distances d_i and d_k along with the distance change Δd are summarized

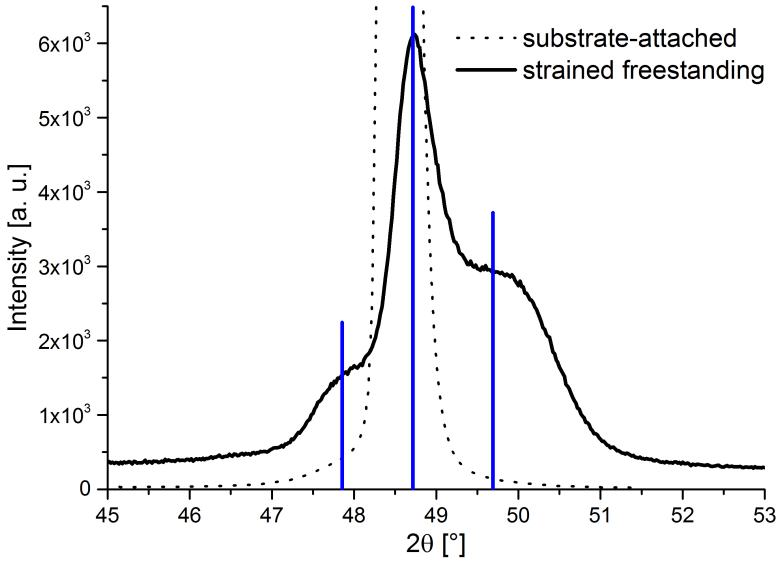

Figure 3: XRD data of sample A1 before and after straining.

in Table 1.

The results indicate growth of individual martensite variants on expense of others - enlargement of variants with one of the longer a-axes, the easy axes of magnetization of fct Fe_7Pd_3, in-plane causes the compression of neighboring variants with the shorter c-axis in-plane and vice versa. The overall distance between the first and the last analyzed twin boundary does not change within its error limits so that the observed distance changes between the individual

Table 1: Variation of distances between twin boundaries A to E by comparing the results for the measurement points i and k at 9.8 and 11.6 % strain, respectively.

	d_i [nm]	d_k [nm]	Δd
AB	364.5 ± 1.5	369.4 ± 1.6	$+4.9 \pm 2.2$
BC	178.7 ± 2.2	173.6 ± 1.4	-5.1 ± 2.6
CD	106.1 ± 1.5	103.2 ± 1.6	-2.9 ± 2.2
DE	70.6 ± 1.3	75.5 ± 2.0	$+5.0 \pm 2.3$
AE	719.9 ± 2.4	721.8 ± 1.5	$+1.9 \pm 2.8$

boundaries state twin boundary movement. These unsteady changes in neighbored twin boundary distances arose from the direction of film straining which was carried out parallel to the visible twinning structures. Due to this, an arbitrary change of film width and height is expected, i.e. compression or widening of individual twin boundary distances cannot be predicted.

Moreover, the performed straining measurements allowed to determine stress-strain curves which were used to calculate the Young's moduli of the specimens. The values for samples clamped on the tensile stage without underlaying plastic wrap are shown in Table 2 and vary strongly due to significant differences in surface structure. SEM and AFM pictures of the analyzed samples permit to distinguish between the surface texture of specimens A2 and A3 with relatively low elastic moduli and specimen A4 with the highest value received. Former show numerous remarkably large grooves with diameters of several μm (see Fig. 2c). Additionally, some surface canyons are broadened compared to other samples. In contrast, the surface of specimen A4 shows more but altogether smaller and less deep canyons and grooves (see Fig. 2d). These surface conditions affect the stress concentration experienced by the connected film at the bottom of the canyons and grooves resulting in higher local stresses and lower elastic moduli for films with less smooth surfaces. Thus, varying surface morphology causes the relatively broad range of determined Young's moduli.

Besides, a drastic lattice softening was already monitored in bulk [12] and freestanding [13] samples with a composition around Fe_7Pd_3. For the latter this was measured by nanoindentation tests and interpreted as an onset of twin boundary motion due to relief of substrate constraints. Compared to the results of these measurements, the values presented here are about a factor two and more smaller. In general, a difference in results is expected because nucleation of twinning dislocations is different perpendicular and parallel to the film surface and nanoindentation tests were carried out out-of-plane, while tensile measurements were performed in-plane. The observation of smaller values in-plane might be connected to the rough surface structure of the specimens which has a stronger impact on film properties in surface plane than in film

Table 2: Selected properties of examined samples at room temperature. sc, pc, TT and SAW denotes single and polycrystalline, tensile test and surface acoustic waves, respectively. The phase appearance refers to the main content.

Sample	Phase	Crystallinity	Method	E [GPa]
M1	fct	sc	TT	3.91 ± 0.01
M2	fct	sc	TT	5.26 ± 0.01
M3	fct	sc	SAW	72.7 ± 12.4
M4	fct	pc	SAW	27.9 ± 6.2
M5	bcc	sc	SAW	217.9 ± 12.4
M6	bcc	pc	SAW	136.5 ± 6.2
A2	fcc	sc	TT	2.19 ± 0.06
A3	fcc	sc	TT	3.79 ± 0.02
A4	fcc	sc	TT	8.29 ± 0.10

depth. Another explanation for the decreased values would be inaccurate sample mounting on the tensile stage, so that the sample cross section experiencing the measured force is decreased resulting in undervalued Young's moduli.

Comparatively, Young's moduli of substrate-attached samples were determined by SAW measurements indicating a significant phase dependancy. The fct-martensitic samples M3 and M4 show relatively low values for substrate-attached Fe_7Pd_3 films but exceed the results of freestanding films by more than a factor of 3. Compared to this, the bcc-martensitic samples M5 and M6 exhibit considerably higher elastic moduli. The reason for this noticeable phase influence is the phase stability of individual transformation steps. The transition between fcc-austenitic and fct-martensitic Fe_7Pd_3 results from lattice softening causing a higher elasticity of the fct phase relative to fcc. In contrast the bcc-martensitic phase, reached after the irreversible transformation from fct via bct to bcc, reveals a high lattice stability and therefore higher elastic moduli.

In addition, temperature dependent SAW measurements of both fct-martensitic samples are presented in Figure 4. The obtained Young's moduli are approximately constant in the temperature regime of fct phase. However, once the

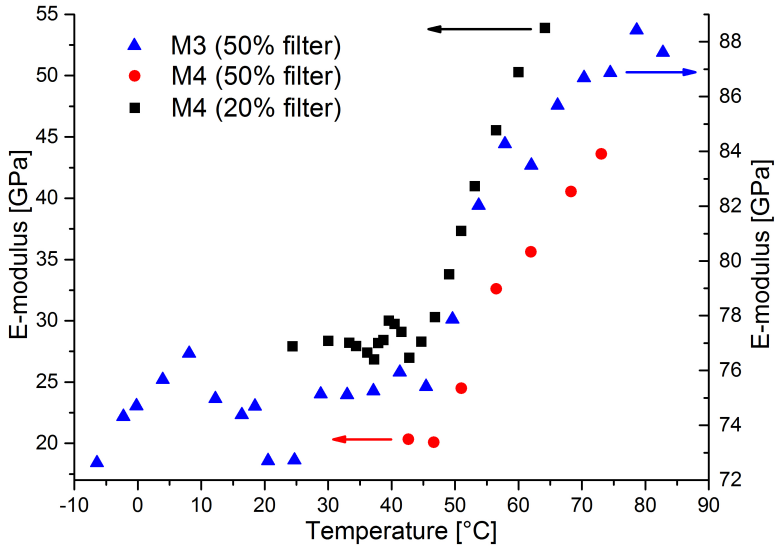

Figure 4: Temperature dependent SAW measurements of single and polycrystalline Fe_7Pd_3 samples with different laser intensity filters.

fcc-fct phase transition temperature of $\approx$ 45 °C is reached, the values increase strongly over a broad temperature range. The rising elastic moduli indicate both a positive temperature coefficient in a wide temperature range above the phase transition temperature [14] and a stiffening of the crystal lattice which occurs during the volume change while transformation from fct to fcc [15]. This increase in elastic moduli, i.e. the lattice stiffening, might be necessary to promote the decrease in anisotropy between *a*- and *c*-axis so that the alloy can traverse the phase transition to fcc [2, 16, 17].

The slope of the increase depends significantly on the intensity of the laser beam used for the SAW measurement. Therefore, measurements on sample M4 were exemplarily performed with different filters to reduce beam intensity to 20 or 50 % of its maximal value, while all other samples were only measured with 50 % intensity. The elastic modulus increases stronger with increasing temperature showing a slope of (1.36 $\pm$ 0.05) GPa/K if the lower laser intensity is used. Compared to this, the measurement at a higher intensity revealed a slope of only (0.89 $\pm$ 0.07) GPa/K. This indicates that at higher laser light intensities,

when stronger surface acoustic waves are created, stiffening is decreased during austenitic phase transformation. This finding might be attributed to the instability in magnetic moment of the d spin band of Fe_7Pd_3 which is countered by an anisotropy change resulting in fct distortion [18]. Higher laser intensities affect that more sample electrons are excited and reach the d band. Therefore, more grains remain in the fct-martensitic phase yielding a lower Young's modulus.

The influence of the d spin band instability became again apparent when the expected Young's moduli were calculated, which are reached after completion of the austenitic phase transition. They correspond to the saturation values of the temperature dependent SAW measurements and were determined by sigmoidal Boltzmann fitting. For M4 this calculation resulted in 57.1 GPa and for M3 in 87.4 GPa, differing considerably from previously published values [13]. Interestingly, the ratio between these saturation values is in accordance with the ratio between the moduli of the measured bcc samples M5 and M6.

Besides, the measured values for sample M5 agreed with predictions calculated with molecular dynamics simulations for martensitic samples [13]. The average value out of 11 SAW measurements given in Table 2 as well as one differing result of (251.2 ± 12.4) GPa coincide very well with the simulated values for $E_{[001]}$ of 220 GPa and $E_{[100],[010]}$ of 251 GPa.

Moreover, the determined Young's moduli at room temperature for single and polycrystalline samples differ significantly. This might be related to sample character, i.e. crystallinity. In polycrystalline samples, grains which are strongly misaligned to the straining direction rotate to maximize deformation strain in this direction in order to minimize their total free energy [19]. Therefore, polycrystalline samples are softer and show a smaller elastic modulus than single crystalline samples.

In summary, we achieved to monitor in-situ the stress-induced martensitic phase transition in 500 nm thin Fe_7Pd_3 films by performing tensile experiments in combination with SEM. At the beginning of plastic film deformation, twin boundaries appeared on the film surface. During further straining, changes in boundary distances were discovered indicating movement of twinning structures

of several nm and twin variant growth.

Further tensile measurements allowed to determine Young's moduli values between 2.2 and 8.3 GPa for freestanding Fe_7Pd_3 thin films varying because of differences in surface morphology. Besides, SAW measurements on substrate-attached samples showed significantly higher values due to substrate constrains. For substrate-attached samples no notable impact of surface morphology on elastic properties was observed. Instead, the influence of phase stability and phase transition characteristics resulted in differing Young's moduli for bcc- and fct-martensitic films and for single and polycrystalline samples, respectively.

We acknowledge funding from the German Science Foundation (DFG), project MICROPUMP and the Translational Center for Regenerative Medicine Leipzig. This work was partially performed within the Leipzig Graduate School of Natural Sciences (BuildMoNa), established within the German Excellence Initiative by the DFG. We further thank Dr. J. Gerlach for the XRD measurement of the strained specimen A1, Dr. A. Arabi-Hashemi for XRD measurements of samples M3 - M6 and F. Lehnert for profilometer measurements.

[1] K. Ullakko, J. K. Huang, C. Kantner, R. C. O'Handley, V. V. Kokorin, Appl. Phys. Lett. 69 (1996) 1966. doi:10.1063/1.117637.

[2] J. Cui, T. W. Shield, R. D. James, Acta Mater. 52 (2004) 35. doi:10.1016/j.actamat.2003.08.024.

[3] Y. Ma, M. Zink, S. G. Mayr, Appl. Phys. Lett. 96 (2010) 213703. doi:10.1063/1.3435260.

[4] A. A. Likhachev, K. Ullakko, Phys. Lett. A 275 (2000) 142. doi:10.1016/S0375-9601(00)00561-2.

[5] A. A. Likhachev, A. Sozinov, K. Ullakko, Mater. Sci. Eng. A 378 (2004) 513. doi:10.1016/j.msea.2003.10.353.

[6] H. Kato, Y. Liang, M. Taya, Scr. Mater. 46 (2002) 471. doi:10.1016/S1359-6462(02)00010-6.

[7] L. Kühnemund, T. Edler, I. Kock, M. Seibt, S. G. Mayr, New J. Phys. 11 (2009) 113054. doi:10.1088/1367-2630/11/11/113054.

[8] I. Kock, T. Edler, S. G. Mayr, J. Appl. Phys. 103 (2008) 046108. doi:10.1063/1.2875306.

[9] T. Edler, S. Hamann, A. Ludwig, S. G. Mayr, Scr. Mater. 64 (2011) 89. doi:10.1016/j.scriptamat.2010.09.013.

[10] T. Edler, S. G. Mayr, Adv. Mater. 22 (2010) 4969. doi:10.1002/adma.201002183.

[11] D. Schneider, B. Schultrich, H.-J. Scheibe, H. Ziegele, M. Griepentrog, Thin Solid Films 332 (12) (1998) 157 – 163. doi:10.1016/S0040-6090(98)00988-2.

[12] F. Xiao, T. Fukuda, T. Kakeshita, Acta Mater. 61 (2013) 4044–4052. doi:10.1016/j.actamat.2013.03.025.

[13] Y. Ma, S. G. Mayr, Acta Mater. 61 (2013) 6756. doi:10.1016/j.actamat.2013.07.048.

[14] T. Nakayama, M. Kikuchi, K. Fukamichi, J. Phys. F: Met. Phys. 10 (1980) 715. doi:10.1088/0305-4608/10/4/022.

[15] M. Stipcich, L. Mañosa, A. Planes, M. Morin, J. Zarestky, T. Lograsso, C. Stassis, Phys. Rev. B 70 (2004) 054115. doi:10.1103/PhysRevB.70.054115.

[16] S. Muto, R. Oshima, F. E. Fujita, Scripta Metall. 21 (4) (1987) 465–468. doi:10.1016/0036-9748(87)90182-7.

[17] S. Muto, R. Oshima, F. Fujita, Acta Metall. Mater. 38 (4) (1990) 685–694. doi:10.1016/0956-7151(90)90224-5.

[18] J.-P. Kuang, M. Kontani, M. Matsui, K. Adachi, Physica B+C 149 (1-3) (1988) 209–216. doi:10.1016/0378-4363(88)90243-4.

[19] R. Albers, R. Ahluwalia, T. Lookman, A. Saxena, Comput. Appl. Math. 23 (2004) 345 – 361.